

**REPORT DOCUMENTATION PAGE**

Public reporting burden for this collection of information is estimated to average 1 hour per response, including the time for reviewing the data needed, and completing and reviewing this collection of information. Send comments regarding this burden estimate or any other aspect of this collection of information, including suggestions for reducing this burden to Department of Defense, Washington Headquarters Services, Directorate for Information Operations and Reports, 1215 Jefferson Davis Highway, Suite 1204, Arlington, VA 22202-4302. Respondents should be aware that notwithstanding any other provision of law, no person shall be subject to a penalty for failing to comply with a collection of information if it does not display a currently valid OMB control number. PLEASE DO NOT RETURN YOUR FORM TO THE ABOVE ADDRESS.

 ding  
ay, Suite

0293

<b>1. REPORT DATE (DD-MM-YYYY)</b> 11-05-2004		<b>2. REPORT TYPE</b> Final Technical Report		<b>3. DATES COVERED (From - To)</b> 01-06-2001 to 30-11-2003	
<b>4. TITLE AND SUBTITLE</b>  Dynamics of Plasma Surface Interactions				<b>5a. CONTRACT NUMBER</b>	
				<b>5b. GRANT NUMBER</b> F49620-01-1-0412	
				<b>5c. PROGRAM ELEMENT NUMBER</b>	
				<b>5d. PROJECT NUMBER</b>	
<b>6. AUTHOR(S)</b>  Dennis C. Jacobs				<b>5e. TASK NUMBER</b>	
				<b>5f. WORK UNIT NUMBER</b>	
				<b>8. PERFORMING ORGANIZATION REPORT</b>	
<b>7. PERFORMING ORGANIZATION NAME(S) AND ADDRESS(ES)</b>  University of Notre Dame 511 Main Building Notre Dame, IN 46556				<b>10. SPONSOR/MONITOR'S ACRONYM(S)</b> AFOSR/NL	
<b>9. SPONSORING / MONITORING AGENCY NAME(S) AND ADDRESS(ES)</b>  Attn: Dr. Michael R. Berman AFOSR/NL 4015 Wilson Blvd., Rm. 713 Arlington, VA 22203-1954				<b>11. SPONSOR/MONITOR'S REPORT NUMBER(S)</b>	
<b>12. DISTRIBUTION / AVAILABILITY STATEMENT</b>  Approved for public release, distribution unlimited.					
<b>13. SUPPLEMENTARY NOTES</b> The views, opinions and/or findings contained in this report are those of the author and should not be construed as an official Air Force position, policy, or decision.					
<b>14. ABSTRACT</b>  This project explored specific strategies to augment the plasma density surrounding hypersonic vehicles through a novel solid-state device that provides cold-cathode electron ejection. Successive deposition of metallic, insulating, and metallic nanolayers on a glass support formed a metal-insulator-metal(MIM) device. When a voltage bias was applied, the MIM device delivered hot electrons to the metal/vacuum interface from within the solid. These hot electrons have the potential to stimulate nonthermal chemical reactions at the gas/surface interface or supplement the charge density of a plasma above the device. The emitted electrons had a relatively narrow distribution of kinetic energies that could be tuned by altering the bias potential. Design and electronic performance characteristics are reported for operational MIM devices.					
<b>15. SUBJECT TERMS</b> Deposition, Thin-films, Nanofabrication					
<b>16. SECURITY CLASSIFICATION OF:</b> Unclassified			<b>17. LIMITATION OF ABSTRACT</b>  UL	<b>18. NUMBER OF PAGES</b>  16	<b>19a. NAME OF RESPONSIBLE PERSON</b> Dennis C. Jacobs
<b>a. REPORT</b> Unclassified	<b>b. ABSTRACT</b> Unclassified	<b>c. THIS PAGE</b> Unclassified			<b>19b. TELEPHONE NUMBER (include area code)</b> (574) 631-8023

BEST AVAILABLE COPY

 Standard Form 298 (Rev. 8-98)  
Prescribed by ANSI Std. Z39.18

20040617 062



UNIVERSITY OF  
NOTRE DAME



Department of Chemistry and Biochemistry  
University of Notre Dame  
Notre Dame, IN 46556

---

Air Force Office of Scientific Research  
Plasma Dynamics for Aerospace Applications Theme  
Grant # F49620-01-1-0412  
Final Technical Report  
1 June, 2001 – 30 Nov, 2003

## **Dynamics of Plasma-Surface Interactions**

Dennis C. Jacobs, Ph.D.  
*Principal Investigator*

---

Approved for public release; distribution is unlimited.

---

## Table of Contents

1. Research Objectives .....	5
2. Experimental Approach.....	6
3. Results and Discussion .....	8
3.1 ALUMINUM OXIDE INSULATING LAYER.....	9
3.2 SILICON OXIDE INSULATING LAYER.....	9
3.3 PERFORMANCE OF MIM DEVICES .....	10
4. Summary .....	13
5. References.....	14
6. Personnel Supported.....	15
7. Publications.....	15
8. Interactions/Transitions .....	15
9. Inventions or Patent Disclosures.....	16
10. Honors and Awards .....	16

## Table of Figures

FIGURE 1.	SCHEMATIC DESIGN OF A BIASED MIM DEVICE.	5
FIGURE 2.	SCHEMATIC DIAGRAM OF DEPOSITION CHAMBER.	6
FIGURE 3.	DEPOSITION CHAMBER FOR FABRICATING AND TESTING MIM DEVICES.	7
FIGURE 4.	ARRAY OF MIM DEVICES DEPOSITED ON A GLASS SUBSTRATE.	8
FIGURE 5.	DIFFERENTIAL CONDUCTANCE ACROSS $\text{Ti/SiO}_2/\text{Au}$ MIM DEVICE AS A FUNCTION OF APPLIED VOLTAGE. POSITIVE AND NEGATIVE VOLTAGE RAMPS SHOW SIMILAR BEHAVIOR.	10
FIGURE 6.	CURRENT OF ELECTRONS EJECTED INTO THE VACUUM AS A FUNCTION OF VOLTAGE APPLIED ACROSS THE MIM.	11
FIGURE 7.	ENERGY DISTRIBUTIONS OF ELECTRONS EMITTED FROM A $\text{Ti/SiO}_2/\text{Au}$ MIM FOR A SERIES OF APPLIED VOLTAGES ACROSS THE M-I-M DEVICE.	12
FIGURE 8.	AFM IMAGES OF THE Au FILM ON THE SURFACE OF THE MIM DEVICE. (A) 20 NM Au IS EVAPORATED DIRECTLY ONTO THE $\text{SiO}_2$ INSULATING LAYER. (B) 20 NM Au IS EVAPORATED ONTO 2.5 NM Ti LAYER WHICH IN TURN IS EVAPORATED ONTO THE $\text{SiO}_2$ INSULATING LAYER.	13

## 1. Research Objectives

The development of many advanced technologies for aerospace applications (e.g., drag reduction, electromagnetic cloaking, combustion enhancement, and magneto gas dynamic control) relies on a weakly ionized plasma flow around the vehicle.<sup>1</sup> To help realize this goal, experiments were performed to develop a novel solid-state device capable of providing cold-cathode electron ejection. The Metal-Insulator-Metal (MIM) heterostructure delivers ballistic hot electrons to the surface from the solid side of the gas/surface interface.<sup>2</sup> Encasing the surface of a hypersonic vehicle with functioning MIM devices could increase the electron density in the boundary layer surrounding the vehicle.

The basic design of the M-I-M device is shown in Figure 1. When the metal overlayer is biased positive relative to the metal underlayer, electron transport through the insulating layer occurs. The objectives of this research grant were to fabricate operational MIM devices and to measure the efficiency and kinetic energy distribution of electrons emitted from the device.

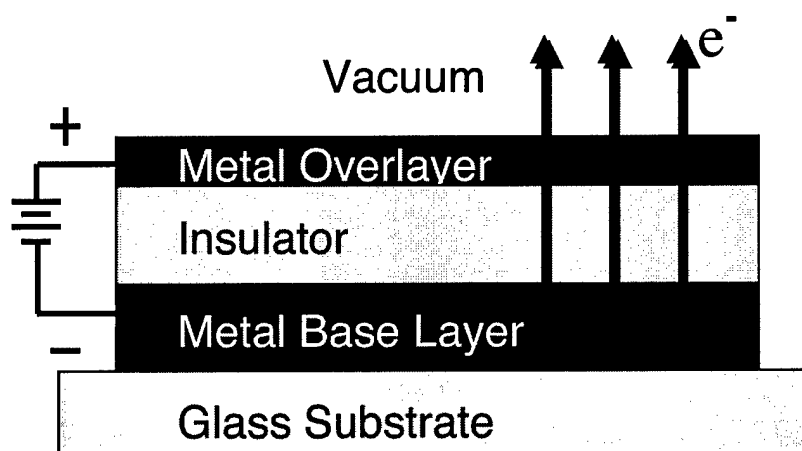


Figure 1. Schematic design of a biased MIM device.

## 2. Experimental Approach

MIM devices were fabricated in a novel deposition chamber where metal evaporation, oxide formation, and device testing are conducted *in situ*. Fabrication of multiple MIM devices on a wafer requires a versatile vacuum chamber for patterning metallic and insulating layers in sequence. Figure 2 shows the design of our experimental apparatus. The chamber contains a magnetron sputter deposition source, a five-pocket metal evaporation source, a two-stage deposition chamber, and the necessary pumps, valves, and electronics. Through the load-lock entry system, a clean substrate is introduced into the apparatus. The metal underlayer is evaporated through a translatable mask while simultaneously monitoring, with Å-resolution, the layer thickness through a quartz-crystal microbalance. Similarly, the insulating oxide layer is deposited, and then finally, a second metal layer is evaporated on top of the insulating layer. The composition and thickness of each metal layer can be systematically varied under

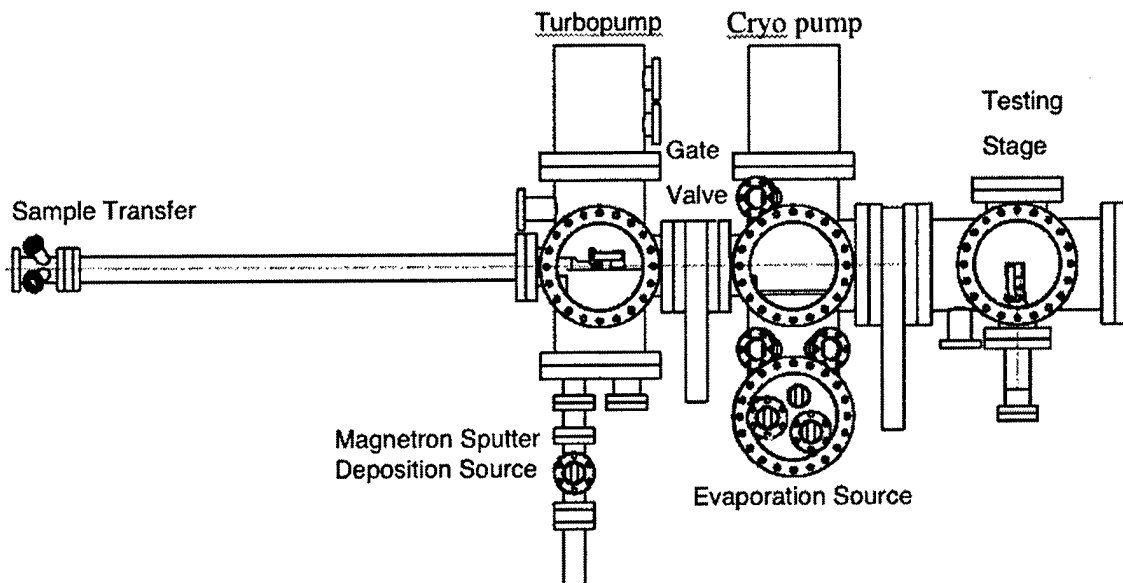
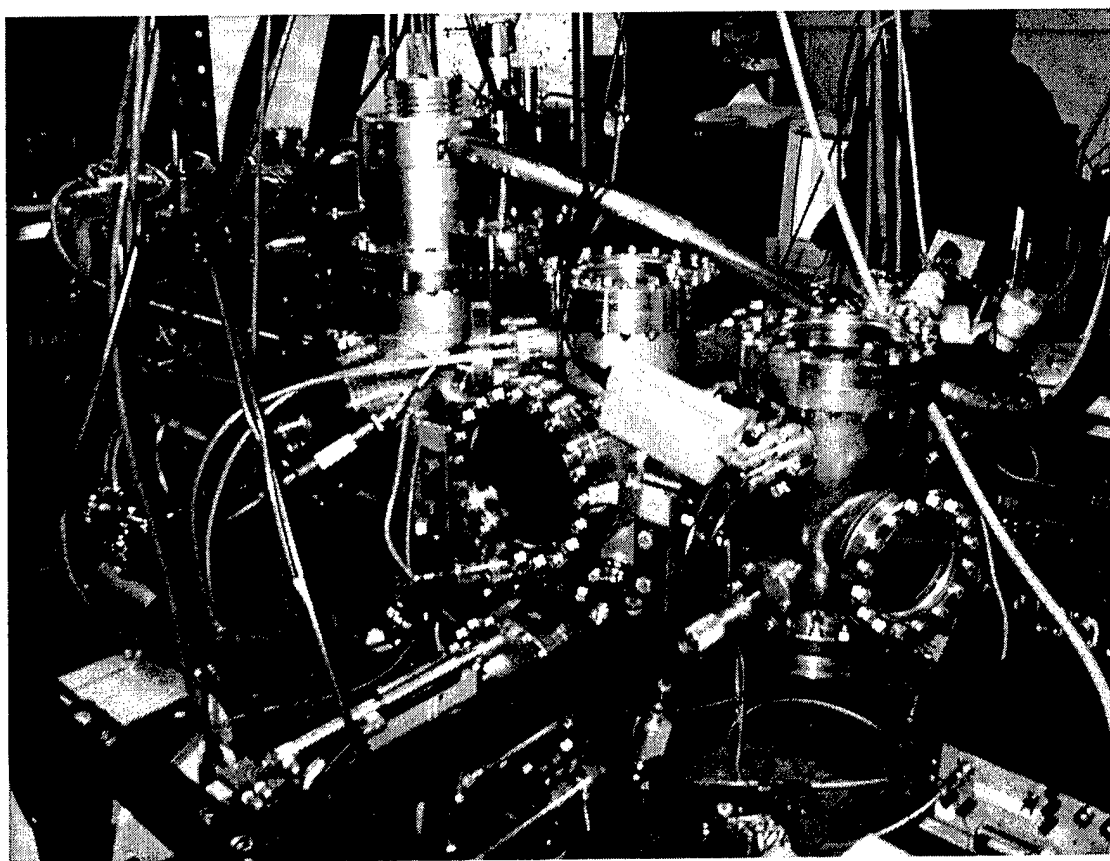


Figure 2. Schematic diagram of deposition chamber.

computer control. After the device is fully fabricated, it can be immediately tested for electron emission *in situ*. A Faraday cup collects the total emission current as a function of bias voltage, and a small hemispherical-sector electrostatic analyzer disperses the electrons to record an energy distribution.

The performance of MIM devices is evaluated by measuring the current density and energy distribution of emitted electrons as a function of the applied bias. Design optimization of the MIM structures entails understanding how device performance is affected by the thickness and composition of the metal and insulating layers.



**Figure 3.** Deposition chamber for fabricating and testing MIM devices.



### 3. Results and Discussion

MIM devices have been fabricated by two methods and subsequently tested for and demonstrated electron emission. The first design involved a 50-nm Al film evaporated onto a glass substrate, which was followed by aqueous anodization *ex situ* to form approximately a 24-nm thick  $\text{Al}_2\text{O}_3$  insulating layer. The outer conducting layer was formed first with a thin Ti film (5.0 nm) that augmented the adhesion of the final, exterior Au layer (20-nm thick). The second family of MIM devices was constructed solely using evaporation techniques. The first metal layer was 20 nm of Ti evaporated onto a glass substrate, followed by evaporation of  $\text{SiO}_2$  at a thickness of 20-50 nm. The final outer layer was 20 nm of evaporated Au.

To streamline the process of identifying optimal fabrication conditions for electron emission and device longevity, we have adopted a combinatorial design approach, which can be seen in Figure 4. Each device is fabricated differently to have its own unique set of properties; consequently, each device must be tested individually. The electrodes can be biased in combinations to activate only one MIM device at a time. By fabricating a series of different MIM devices on a single substrate, a more accurate comparison can be made between the performance of devices grown with varied layer thicknesses.

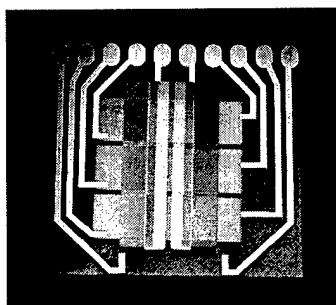
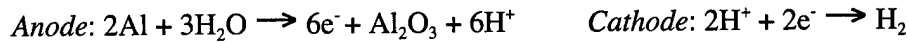


**Figure 4.** Array of MIM devices deposited on a glass substrate.

### 3.1 Aluminum oxide insulating layer

The first class of MIM devices were fabricated with a  $\text{Al}_2\text{O}_3$  insulating layer. Anodization was performed *ex situ* after evaporation of a 75.0 nm Al film onto a glass substrate. Anodization is an electrochemical method of creating a thin insulating film. For this experiment, the Al anode is oxidized by passing a constant current through an aqueous 0.1M ammonium tartrate solution to an inert Pt cathode, generating the following two half reactions:



The thickness,  $d_{ox}$ , of the oxide can be estimated based on the final anodization potential,  $V_{anod}$ , according to the equation

$$d_{ox}(\text{nm}) = 1.3 \times V_{anod} + 2.0 \text{ nm.}^3$$

In the experiment, the final anodizing voltage was approximately 17 volts, which yields and insulator thickness of approximately 24 nm. After the anodization procedure, the substrate was cleaned with ethanol, dried with Ar gas, and then reinserted into the vacuum chamber to complete the fabrication. The metal overlayer in this device consisted of an evaporated 5.0 nm Ti layer, that serves to enhance the adhesion of the final evaporated Au layer (20.0 nm thick).

### 3.2 Silicon oxide insulating layer

The second family of functioning MIM designs was fabricated and tested entirely *in situ* using evaporation methods exclusively. The first metal layer was 20.0 nm of Ti evaporated onto a glass substrate, followed by evaporation of  $\text{SiO}_2$  at a thickness of 20-50 nm. The final outer layer was 20 nm of evaporated Au. To help wet the silicon oxide layer, a 2.5 nm layer of titanium was sometimes evaporated prior to the gold layer.

### 3.3 Performance of MIM devices

The conducting metal layers of the nanolaminate device were biased such that hot electrons tunneled from the base metal layer through the oxide layer to the conducting overlayer.<sup>4</sup> The differential conductance ( $dI/dV$ ) across the Ti/SiO<sub>2</sub>/Au device varies dramatically with applied voltage. Figure 5 shows how the device demonstrates negative differential conductance when the applied bias is between 5 – 6 Volts. This implies that an increase in applied voltage leads to a decrease in the current flowing across the device.

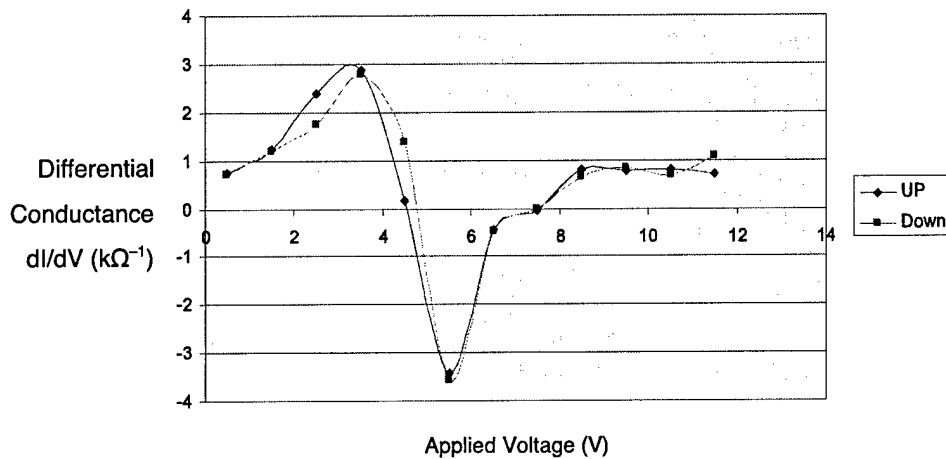


**Figure 5. Differential conductance across Ti/SiO<sub>2</sub>/Au MIM device as a function of applied voltage. Positive and negative voltage ramps show similar behavior.**

A portion of the hot electrons was emitted from the metal/vacuum interface. Figure 6 shows how the emission current depends on the voltage applied across the metal layers. No electron current is expected below 5 V, because the electron energy must exceed the workfunction of the gold surface. No appreciable emission current was observed until a 10 V bias was applied, at which point the emission current began to increase significantly. As the bias potential was ramped to 15 V, the emission current increased by many orders of magnitude. This nonlinear behavior underscores the nonclassical

nature of the tunneling phenomenon associated with MIM technology.<sup>5</sup> The maximum emission current density measured from most MIM devices is in the range of 1 mA/m<sup>2</sup>.

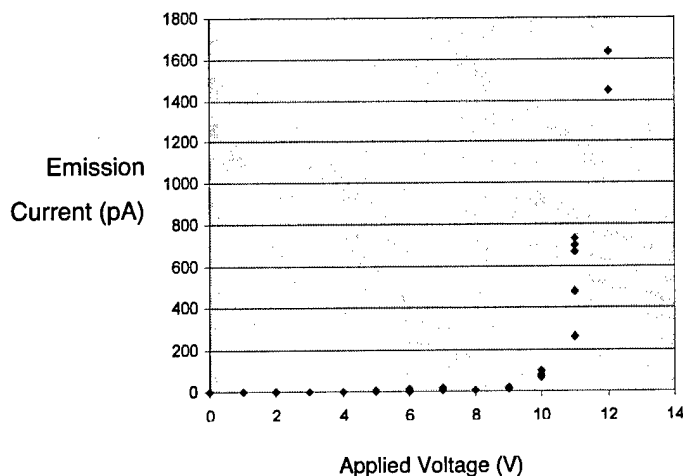


**Figure 6. Current of electrons ejected into the vacuum as a function of voltage applied across the MIM.**

The exoelectron energy distributions are measured with a hemispherical-sector electrostatic energy analyzer. Ideally, the electrons emitted by the MIM device would be monoenergetic, but many electrons undergo scattering in the lattice, leading to a distribution of energies.. The energy distribution of the emitted electrons shown in Fig. 7 suggests that a significant portion of the distribution is associated with quasi-ballistic electrons (minimal energy loss), and the remainder represents those that have undergone significant inelastic scattering within the solid. Theoretically, the maximum energy with which a ballistic electron would escape the surface equals the applied bias potential minus the work function ( $\Phi$ ) of the exterior metal (in this case Au, which has  $\Phi = 5.5$  eV). For example, a 10 V bias would produce exoelectrons with kinetic energies below 4.5 eV. This is consistent with the data in Fig. 7 if one considers the instrumental broadening of the energy distribution.